ELSEVIER

Journal of Nuclear Materials 258–263 (1998) 1533–1539

journal of nuclear materials

Section 6.3. SiC/SiC composites

Light ion irradiation creep of SiC fibers in torsion

R. Scholz *

Institute of Advanced Materials, CEC Joint Research Centre, TP202, 21020 Ispra (Va), Italy

Abstract

Creep tests were conducted in torsion on TEXTRON type SCS-6™ silicon carbide (SiC) fibers during irradiation with 14 MeV deuterons for 450°C, 600°C and 800°C. The fibers, produced by chemical vapor deposition (CVD), should be representative of the chemical vapor infiltrated (CVI) matrix of a SiC/SiC composite. SiC is known to undergo irradiation induced swelling which occurs without an incubation dose for temperatures below about 1000°C [R.J. Price, J. Nucl. Mater. 33 (1969) 17]. Such swelling in SiC may mask the irradiation creep strain in a tensile experiment, but plays a minor role in torsional creep tests. The torsional irradiation creep curves are characterized by long lasting strain transients during which the creep rate slows down before reaching approximately constant values. The steady state torsional creep rate $\dot{\gamma}_s$ exhibited a linear dependence on stress and particle flux and it decreased when the temperature was increased. The temperature dependence of $\dot{\gamma}_s$ in the range 450–800°C is similar to that of swelling for neutron irradiated SiC.

1. Introduction

SiC matrix composites are being considered as structural materials for the first wall and blanket of nuclear fusion reactors [1]. A commonly used production procedure for this material is the chemical vapor infiltration (CVI) technique. A detailed analysis of the SiC matrix microstructure showed that polycrystalline SiC produced by CVI is basically the same material as polycrystalline SiC produced by chemical vapor deposition (CVD) [2]. Therefore, the TEXTRON SCS-6 fiber, produced by a CVD procedure, may be considered as representative of a SiC/SiC composite matrix produced by CVI.

The effects of high-energy particle irradiation on the mechanical properties of SiC, SiC fibers or SiC composites have been determined predominantly in post-irradiation tests [3,4]. Post-irradiation bend stress relaxation creep of SiC has been studied by Price [5] after fast neutron irradiation for temperatures in the range 780–1130°C. Price observed a temperature independent irradiation creep deformation that exceeded thermal creep over the range from 780°C to 1100°C and which exhibited linear stress dependence. The irradiation-induced strain increase reported by Zhu and Jung [6] during irradiation with 10.7 MeV protons in the temperature range 235–505°C with applied tensile stresses of 20–100 MPa showed a square root dose dependence and almost no stress dependence. The 0.3–0.5 linear strain was ascribed to volume swelling. SiC is known to undergo isotropic expansion which, in the temperature range below 1000°C, occurs without an incubation dose and, depending on temperature, saturates rapidly within a total dose of less than 0.5 dpa. The magnitude of linear swelling observed after saturation decreases with increasing irradiation temperature from ca. 1% at room temperature to 0.05% at 1000°C [7].

For small irradiation doses, to which light ion creep tests are usually limited, the magnitude of swelling observed for SiC is sufficient to mask the irradiation creep strain in tension for temperatures below 600°C. In torsion creep tests under the same irradiation conditions, swelling effects play a minor role.

2. Experimental details

2.1. Fiber structure and specimen preparation

The single fiber specimens were made from TEXTRON type SCS-6™ silicon carbide fibers (Textron

* Tel.: +39-332 789 260; fax: +39-332 789 434; e-mail: scholz@jrc.it.

0022-3115/98/$19.00
PII: S0022-3115(98)00216-5

Specialty Materials, Lowell, MA, USA). Other studies of the SCS-6 fiber showed that the fibers consisted of a 33 μm diameter carbon core covered by a thin pyrolitic graphite layer on which the SiC layer of 50 μm thickness was deposited. A final outside coating of 3 μm thickness [8,9] was then deposited. The resulting fiber diameter amounts to about 142 μm. The SiC fiber sheath consists of four concentric regions around the carbon core, see Fig. 1. The transition from one region to the next is characterized by an increase in grain size and the degree of preferred orientation of the grains in the radial direction. The outer SiC region which consists of columnar, 8–12 μm long β-SiC grains lying in radial direction with (1 1 1) preferred orientation, is about 35 μm thick. Region four consists of almost perfectly stochiometric β-SiC while the inner regions 1–3 have 10–20% excess carbon. The outside, 3 μm thick carbonaceous coating has three sublayers. The outermost and the innermost layer are carbon-rich and contain SiC crystallites. The middle sublayer is pure carbon with weakly bonded graphite planes parallel to the fiber surface.

An analysis of the fiber fracture surface after fatigue tests in torsion indicated that there were two weak interfaces where debonding had occurred: the inside coating close to the carbon core and within the outer carbon coating [10]. Therefore, the maximum shear stress τ_m and shear strain γ_m are calculated for a hollow tube by adopting the values for the inside radius R_2 and outside radius R_1 of the SiC sheath: $\tau_m = 2M/(\pi R_1^3)$ and $\gamma_m = \phi R_1/L$, where M stands for the applied torque, and $\phi = 2ML/[\pi G(R_1^4 - R_2^4)]$ is the twist angle and G the shear modulus. Thus $\gamma_m = \tau_m/G[R_1^4/(R_1^4 - R_2^4)]$.

Both ends of a ca. 8 cm long SCS-6 fiber were Ni-plated by a Ni-electroplating process. The central fiber segment of 8 mm, the gauge length over which the rotation occurs, when a torque is applied to the specimen, remained unplated. The Ni-plated ends of the specimen were fixed in the grips of the creep machine without inducing any additional deformation on the fiber in the vicinity of the gauge length.

2.2. Experimental procedure

The specimens were heated to their creep temperature by a direct current and cooled by flowing helium which is held at constant velocity and a temperature of 20°C. The dpa rate was calculated from the difference in electric heating power input for beam on/off conditions with the aid of the TRIM-code [11] by assuming an overall displacement energy of 38.5 eV for the material [12].

Before the irradiation creep tests, the specimens were exposed, for 10–48 h, to the same stress and temperature conditions imposed during the irradiation in order to exhaust strain transients of thermal origin. For all tests, the strain rate was zero at the end of this period, the strain accumulated was completely anelastic, i.e. recoverable after removal of the applied torque. Even at temperatures higher than 950°C, the time dependent strain accumulated during the first 100 h of creep was mainly anelastic. More details regarding the experimental set-up, temperature and strain measurement are given elsewhere [13].

The dependence of the irradiation induced creep rate on applied stress, flux, and temperature were examined for an irradiation with 14 MeV deuterons. Their penetration depth in SiC, calculated with the TRIM-code, amounts to about 0.5 mm. The maximum inhomogeneity in dpa-rate between the inlet and the outlet surface of the specimen in beam direction is less than 12%.

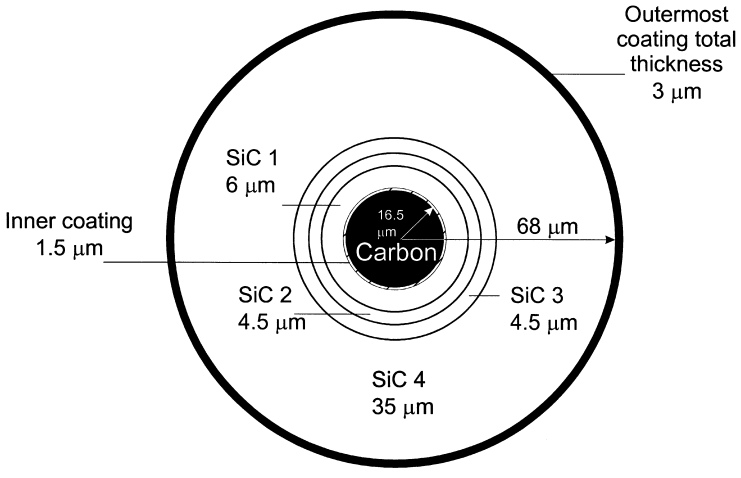

Fig. 1. Concentric layer structure of the Textron SCS-6 fiber. The approximate thickness of each region is given in the figure (from Ning and Pirouz [9]).

3. Results

3.1. Stress dependence

Fig. 2 shows the irradiation creep curves for two different specimens at 600°C. The strain is plotted versus the accumulated dose. A maximum shear stress of 320 MPa was applied to the first specimen. The creep rate continuously decreases from the beginning of the irradiation and reaches steady state after about 0.04 dpa. A maximum shear stress of 80 MPa was initially applied to the second specimen. As a function of dose, the creep curve exhibits similar features: after a transient phase, the creep rate reaches a nearly constant value. The slopes of the straight lines drawn in Fig. 2 are equal to the steady state creep rate $\dot{\gamma}_s$ for each stress level. Assuming that the total irradiation creep strain γ has two components, a transient component γ_t, and a steady state component γ_s, the magnitude of γ_t is given by the intersection of the extrapolated line and the ordinate. Within the limits of extrapolation from the steady state portion of the creep curves, γ_t increases only slightly with stress (Fig. 2). For the second specimen, after the first irradiation period, the applied stress was doubled to 160 MPa. The test was continued, first with the beam off for 14 h to eliminate thermal transients, thereafter under irradiation conditions. There was only a small strain transient at the beginning of the second irradiation period, and the steady state regime was attained almost immediately.

In an attempt to study further the origin of the transient creep strain component, a third specimen was exposed to irradiation on two occasions at a temperature of 600°C and a maximum shear stress of 160 MPa: the absolute magnitude of stress was maintained but its direction was reversed (see Fig. 3). This operation can be accomplished simply by inverting the current direction of the electromagnetic loading system. Before each irradiation run, the specimen was exposed to the same loading and temperature conditions maintained during irradiation. In Fig. 3, the strain is plotted as a function of dose. For both runs, the absolute magnitude of the strain-dose relationship is equal, i.e. the large strain transients recur after stress reversal.

In Fig. 4, the quotient $s =$ creep rate/damage rate is plotted versus the applied maximum shear stress. The creep rates are taken as the mean slopes between 0.04 and 0.06 dpa of the creep curves plotted in Figs. 2 and 3. Fig. 4 shows that the steady state irradiation creep rate is a linear function of stress.

3.2. Flux dependence

To examine the effect of a flux change on the irradiation creep rate, the specimen was exposed to irradiation until the steady state irradiation creep regime was attained. At this point, the beam intensity was increased or decreased, while maintaining stress and temperature constant. The difference in beam power input is compensated by adjusting the ohmic heating accordingly. By applying this procedure, the effect of flux changes on the momentary irradiation creep rate of a single specimen can be observed. Fig. 5 shows an example for a test conducted at 600°C and a maximum shear stress of 160 MPa. The shear strain, after having reached the steady state creep regime, is plotted versus time before and after a dose rate change from 1.8×10^{-6} to 4.2×10^{-6} dpa/s, i.e. the flux has been increased by a factor of 2.4. The irradiation creep rate, after the change in beam intensity, increases immediately by the same factor indicating that there is a linear relationship between the steady state irradiation creep rate and the particle flux. A similar

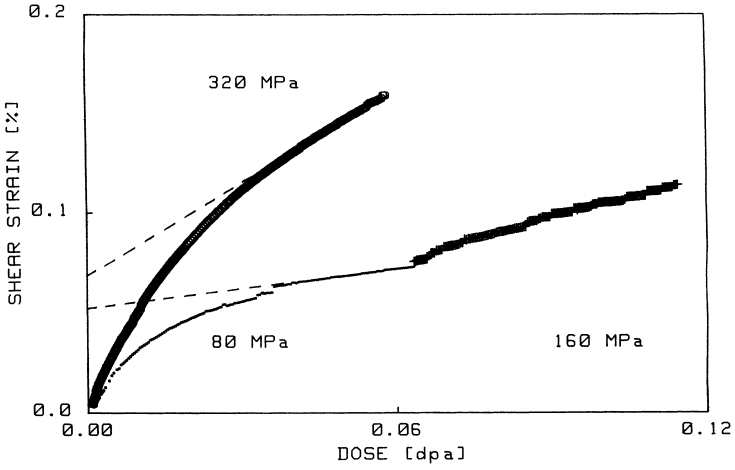

Fig. 2. Maximum shear strain as a function of dose for SCS-6 fiber when maximum shear stresses of 80, 160, 320 Mpa were applied.

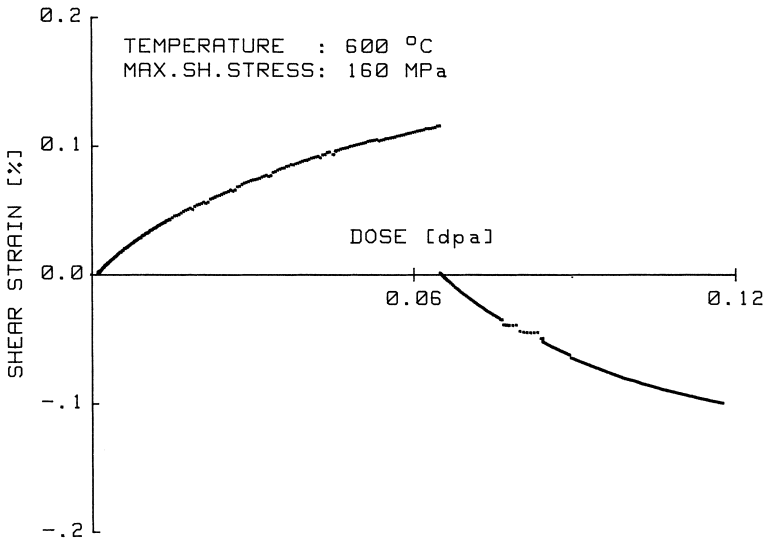

Fig. 3. The effect of stress reversal on the irradiation creep strain.

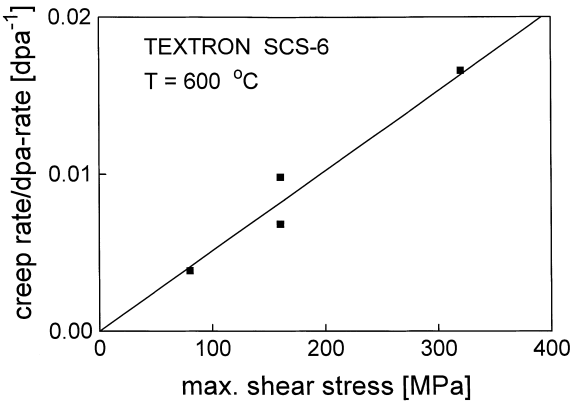

Fig. 4. The effect of stress on the steady-state irradiation creep rate per unit dose.

observation was made after a decrease in flux [10]. Fig. 5 also indicates that there was no strain transient after the flux change. However, both curves, before and after the change in beam intensity, exhibit the characteristic slight negative curvature as was observed for the 'steady state' portion of the creep curves measured at 450°C and 600°C.

3.3. Temperature dependence

In Fig. 6 are plotted the irradiation creep curves measured for a maximum shear stress of 320 MPa at 450 and 600°C. Both quantities, creep strain and creep rate, are higher for the 450°C curve over the whole dose range of 0.06 dpa. This trend was observed for all tests conducted in the temperature interval from 450°C to 800°C. Temperature change tests conducted on a single specimen confirmed this result. In these tests, the sample temperature was changed after having reached the steady state creep regime while keeping all other parameters constant. Fig. 6 shows the strain dose relationship measured for a specimen exposed to irradiation at a temperature of 800°C until a dose of 0.045 was reached. At this point temperature was suddenly lowered to 600°C by reducing the electric heating current. The creep rate, after the drop in irradiation temperature, increases and stays higher for the remainder of the test. All temperature change tests in the range between 450°C and 800°C showed consistent results, i.e. whenever the temperature was lowered the creep rate increased, when the temperature was increased the creep rate decreased.

4. Discussion

4.1. Swelling and irradiation creep

In Fig. 7, the irradiation induced linear swelling behavior of SiC from Ref. [5] is plotted as a function of irradiation temperature (solid squares). The irradiation creep compliance $\kappa =$ (steady state shear strain rate)/(damage rate × max. shear stress), derived from the data plotted in Figs. 3 and 6, are shown as a function of temperature on the same plot (open triangles). Both, linear swelling and irradiation creep compliance, exhibit a similar temperature dependence in the interval from 450°C to 800°C with approximately a linear decrease in linear swelling and torsional creep compliance with increasing temperature. In contrast, the amount of flexural irradiation creep of β-SiC strips irradiated in a fast

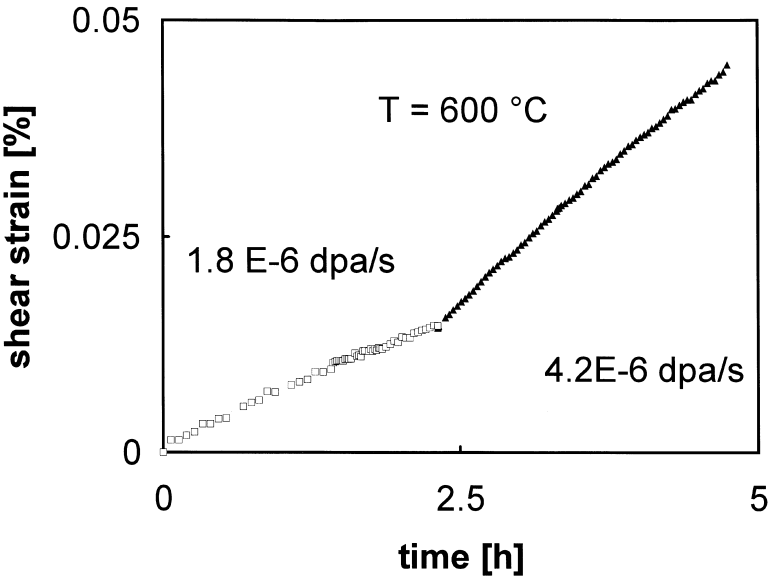

Fig. 5. The effect of flux change on the irradiation creep strain.

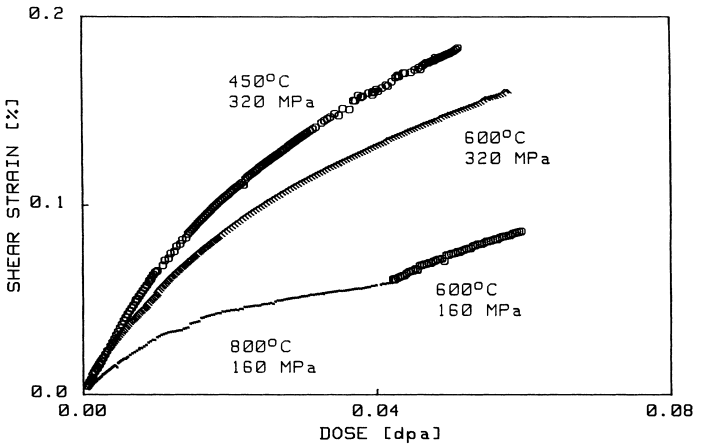

Fig. 6. Creep curves for 450°C and 600°C at a maximum shear stress of 320 MPa. The effect of a change in temperature from 800°C to 600°C. The steady state torsional creep strain induced by irradiation increases if the temperature is decreased.

neutron spectrum up to a fluence of 7.7×10^{25} n/m^2 was independent of temperature in the range 780–1100°C. However, the temperature independent flexural creep compliance estimated by Price was about 5×10^{-13} [Pa^{-1}dpa^{-1}], which is about two orders of magnitude lower than the torsional creep compliance measured for 600°C.

For temperatures below 1000°C, the accumulation of single defects or small defect clusters cause irradiation induced swelling of the material [7]. Among the four possible point defects, which are the vacancy and interstitial of Si and C, according to molecular dynamics simulation [14], only the carbon interstitial is mobile in the range 400–800°C, and the difference in irradiation creep observed in this temperature range may be attributed to the difference in mobility, $v_c = v_o \exp(-E_m/(kT))$, and concentration, c_c, of this point defect. (E_m is the activation energy for migration of the carbon interstitial and the other parameters have their usual meaning). By assuming a diffusion controlled creep mechanism, the irradiation creep rate would be proportional to the product $v_c \cdot c_c$. Since v_c increases with temperature, the concentration of interstitials which are available for the irradiation creep process should drop if the temperature is increased, in order to explain the observed temperature dependence of $\dot{\gamma}_s$.

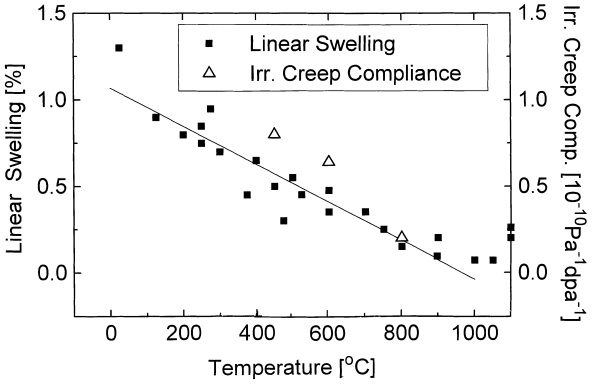

Fig. 7. Linear swelling (Ref. [5]) and torsional irradiation creep compliance κ as a function of temperature. Both quantities drop with temperature.

Since swelling in SiC saturates only after a total dose of about 0.5 dpa, for the doses obtained in the present tests which are smaller than 0.12 dpa, it can be assumed that the concentration of irradiation induced defects have not reached equilibrium conditions. The slight drop in irradiation creep rate which is observed for most creep curves after having reached the 'steady state' regime may be explained with accumulation of immobile vacancies which absorb more and more of the mobile interstitials, such that creep process is slowed down and possibly stopped at higher doses.

4.2. Strain transients

Grain boundary sliding (GBS) is the creep mechanism that has been cited mainly for the interpretation of thermal creep data in polycrystalline ceramic materials. In the study by Dicarlo on AVCO SCS-6 fibers [15], which have a similar structure as the TEXTRON SCS-6 fibers, the strain transients with negative curvature observed in tests conducted at specimen temperatures between 1000°C and 1500°C were interpreted as a GBS effect: by sliding of a grain along another, elastic stresses are built-up which slow down the sliding process and possibly stop it, if they have reached the same magnitude as the external stresses. This argumentation can be adopted in order to explain the strain transients observed in the tests plotted in Figs. 2 and 3. Obviously, if the stress is increased without a relaxation period, a small strain transient is observed in the second irradiation run, since the elastic stresses built-up in the previous run are opposing the external stress. After stress reversal, the elastic stresses built-up previously are relaxed during the intermediate thermal creep periods such that they cannot influence the shape of the second run irradiation creep curve and the strain transient occurs again. If it is assumed that GBS is the underlying microstructural process for the creep process, diffusion of carbon interstitials generated by the irradiation, may control the accommodation process, which is required if coherency of the material is postulated.

5. Conclusions

Irradiation-induced creep has been observed in torsion on the TEXTRON SCS-6™ fiber in the temperature range from 450°C to 800°C during irradiation with 14 MeV deuterons and with applied maximum shear stresses from 80 to 320 MPa. The creep behavior of a SCS-6 fiber, produced by a CVD procedure should be representative of the creep behavior of the CVI matrix in a SiC/SiC composite. Analysis of the measured torsional creep curves indicates that:

i. The total torsional creep strain induced by irradiation has two components: a transient component, γ_t, and a steady state component, $\gamma_s \cdot \dot{\gamma}_s$ depends linearly on the applied maximum shear stress and particle flux and γ_t increases only slightly with stress.

ii. The irradiation induced rate, $\dot{\gamma}_s$ increases if the temperature is lowered in the range from 450°C to 800°C. The temperature dependence of $\dot{\gamma}_s$ is similar to the temperature dependence of swelling determined for SiC after neutron irradiation.

References

[1] L.H. Rovner, G.H. Hopkins, Nucl. Technol. 29 (1976) 274.
[2] L.U. Ogbuji, T.E. Mitchell, A.H. Heuer, J. Am. Ceram. Soc. 64 (1981) 100.
[3] M.C. Osborne, L.L. Snead, D. Steiner, J. Nucl. Mater. 219 (1995) 63.
[4] A. Hasegawa, G.E. Youngblood, R.H. Jones, Fusion Materials Semiannual Progress Report for period ending 31 December, DOE/ER-031/19 (1995) p. 1015.
[5] H.J. Price, Nucl. Technol. 35 (1977) 320.

[6] Z. Zhu, P. Jung, J. Nucl. Mater. 212–215 (1994) 1082-1086.
[7] R.J. Price, J. Nucl. Mater. 33 (1969) 17.
[8] A. Parvizi-Majidi, Fibers and Whickers, in: Material Science and Technology, vol. 13, pp. 27–68.
[9] X.J. Ning, P. Pirouz, J. Mater. Res. 6 (1991) 2234.
[10] R. Scholz, A. Frias Rebelo, F. dos Santos, in: Proceedings of IEA International Workshop on SiC/SiC Ceramic Composites for Fusion Structural Applications, Ispra, Italy, 1996, p. 151.
[11] J.P. Biersack, L.G. Haggmark, Nucl. Instr. and Meth. 174 (1980) 93.
[12] A. El-Azab, N.M. Ghoniem, J. Nucl. Mater. 212–215 (1994) 148.
[13] R. Scholz, J. Nucl. Mater. 212–215 (1994) 530.
[14] H. Huang, N. Ghoniem, J. Nucl. Mater. 212–215 (1994) 148.
[15] J.A. DiCarlo, J. Mater. Sci. 21 (1986) 217.